A label-free immunosensor array using single-chain antibody fragments

Natalija Backmann*, Christian Zahnd†, Francois Huber*, Alexander Bietsch*, Andreas Plückthun†, Hans-Peter Lang*‡, Hans-Joachim Güntherodt*, Martin Hegner*§, and Christoph Gerber*

*National Center of Competence in Research for Nanoscience, Institute of Physics, University of Basel, Klingelbergstrasse 82, CH-4056 Basel, Switzerland; †Institute of Biochemistry, University of Zürich, Winterthurerstrasse 190, CH-8057 Zürich, Switzerland; and ‡IBM Research, Zurich Research Laboratory, Säumerstrasse 4, CH-8803 Rüschlikon, Switzerland

We report a microcantilever-based immunosensor operated in static deflection mode with a performance comparable with surface plasmon resonance, using single-chain Fv (scFv) antibody fragments as receptor molecules. As a model system scFv fragments with specificity to two different antigens were applied. We introduced a cysteine residue at the C terminus of each scFv construct to allow covalent attachment to gold-coated sensor interfaces in directed orientation. Application of an array enabled simultaneous deflection measurements of sensing and reference cantilevers. The differential deflection signal revealed specific antigen binding and was proportional to the antigen concentration in solution. Using small, oriented scFv fragments as receptor molecules we increased the sensitivity of microcantilevers to ≈1 nM.

cantilever arrays | nanomechanics | proteomics

Microcantilever-based sensors have attracted much interest as devices for fast and reliable detection of small amounts of molecules in air and solution. Over the last few years the application of the cantilever sensor concept was extended to the measurements of biocompounds in solution, resulting in a versatile biosensor (1, 2). Because of its label-free detection principle and small size, this kind of biosensor is advantageous for diagnostic applications, disease monitoring, and research in genomics or proteomics (3, 4). Multicantilever arrays would enable the detection of several analytes simultaneously.

The main principle of the cantilever static mode is the transduction of the molecular interaction between analyte and receptors, immobilized as a layer on one surface of a cantilever, into a nanomechanical motion of the cantilever. Biomolecular interactions taking place on a solid-state interface produce a change in surface stress, because of changes in molecular configuration and intermolecular crowding (5). This process results in bending of the cantilever. Microcantilever-based biosensors operated in static mode have been successfully applied for the detection of various molecular interactions such as ssDNA–ssDNA (5–7) or protein–DNA (8, 9). Interactions between proteins were detected with cantilever-based immunosensors, where an antigen was recognized by its cognate antibody randomly immobilized on the sensor surface (10–12).

The most critical step in preparation of any immunosensor is the immobilization of capture molecules on the support, a process where the orientation of the antigen-binding sites toward the analyte in solution plays a key role. Immunoglobulins can be either adsorbed on gold directly (10, 12) or attached covalently to the surface modified with hetero-bifunctional self-assembled monolayers of alkylthiols (11). However, these approaches produce a layer of randomly oriented antibody molecules on the cantilever surface, thereby generating conformational heterogeneity and inactive receptor molecules (13, 14).

As previously shown (13, 15–18), the sensitivity of immunosensors can be improved by both maximizing the degree of functional orientation of the active sites and minimizing the size of antigen-binding molecules (resulting in a denser receptor layer). Thus, the sensitivity of surface plasmon resonance (SPR) and quartz crystal microbalance sensors was significantly improved by using antibody fragments (13, 19), which can be bound covalently to the sensor surface in an oriented manner by using their C-terminal SH groups.

Single-chain Fv (scFv) fragments of an antibody with a molecular mass of ≈28 kDa are the smallest antibody entities comprising an intact antigen-binding site, therefore, still capable of binding antigens with the same affinity (20). Phage and ribosome display techniques (21, 22) allow the in vitro generation of high-affinity scFv molecules against virtually any molecular targets. These receptor molecules can be labeled with tags, including oligo-histidine tags, biotin labels, or unpaired cysteine residues. Thus, scFv fragments provide advantages over intact IgG molecules, such as their minimized size, the possibility for directed and dense immobilization on interfaces, and their ease of production.

In the present study, we tested the applicability of scFv fragments for developing high-sensitivity microcantilever-based immunosensors. Two antibody fragments with specificity to different peptides were covalently immobilized in directed orientation on the gold-coated side of cantilevers by using cysteine introduced at the C-terminal end of the protein constructs reacting with gold. Using scFv fragments as receptor proteins, we achieved at least a 500-fold improvement of the sensitivity of the method as compared with previous studies with randomly oriented IgG molecules (11, 12). Our data were compared with SPR measurements and revealed a similar sensitivity of both label-free detection techniques.

Materials and Methods

Materials. All buffer components were purchased from Sigma-Aldrich. The plasmid DNA encoding G9-scFv (unpublished data) was kindly provided by B. Luginbühl (University of Zürich). The antigenic fusion protein MBP13_6-GCN4 was kindly provided by K. Binz (University of Zürich).

Cloning, Expression, and Purification of Thiolated scFv Fragments. To attach a free thiol group at the C-terminal end of antibody fragments, the scFv genes of antibody fragments C11L34S (23) and G9 were cloned into the expression vector pDR01/cysII, a derivative of the plasmid pAK400 (24), containing a C-terminal His-6 tag followed by a cysteine residue. The scFv proteins, referred to as C11L34Scys and G9cys (molecular mass 28 kDa), were expressed in *Escherichia coli* SB536 as described (23). Briefly, the clones were grown in 1 liter of SB medium (20 g
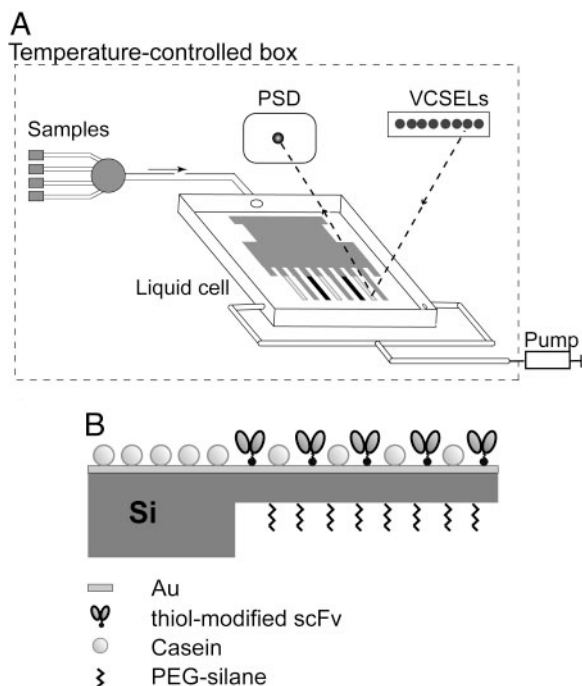

BIOPHYSICS

Fig. 1. Measurement setup and sensor functionalization. (*A*) Schematic drawing of the sensor instrument: optical read-out system comprising vertical cavity surface emitting lasers (VCSELs), a position sensitive detector (PSD), liquid cell (40 μl) with mounted eight-cantilever array, syringe pump, and valve selector connected to liquid samples. The incident laser beam is focused at the apex of the cantilevers and the reflected light is detected with a PSD. (*B*) Side view of a gold-coated silicon cantilever functionalized with cysteine-modified scFv antibody fragments. Sensing and reference cantilevers are coated with C11L34cys and G9cys proteins, respectively.

trypton, 10 g yeast extract, 5 g NaCl) supplemented with 1% glucose, 20 mM K_2HPO_4, 4 mM $MgSO_4$, and 50 μg/ml chloramphenicol at 25°C. Cells were induced at an OD_{600} of 0.7–0.8 and harvested by centrifugation after incubation for 5 h at 25°C. Soluble scFv constructs were purified from the complete cell lysate by immobilized metal ion affinity chromatography, followed by affinity chromatography on an antigen column as described (25). Purified proteins were dialyzed against Hepes-buffered saline (HBS) buffer (20 mM Hepes/150 mM NaCl, pH 7.5). From 1 liter of bacterial culture ≈0.5 mg of purified protein was isolated. Gel electrophoresis showed that both scFv fragments were monomeric.

ELISA. Ninety-six-well plates (Nunc) were coated with neutravidin in a concentration of 1 μg/ml in PBS (pH 7.4). After blocking with 2% BSA, biotinylated GCN4 peptide was added in a concentration of 50 ng/ml (10^{-8} M) and incubated for 45 min. After washing, cysteine-modified scFv fragments were added alone or in a mixture with an excess of free GCN4 peptide as competitor, to test specific binding. The final concentration of scFv fragments and the peptide in the mixture was 50 and 100 nM, respectively. Bound scFv fragments were detected by using the mouse monoclonal anti-tetra-histidine antibody (Qiagen, Valenica, CA) and a polyclonal goat anti-mouse IgG/alkaline phosphatase conjugate. The enzymatic reaction was developed with *p*-nitrophenyl phosphate. The absorbance at 405 nm was measured.

Sensor Instrument. The deflection of microcantilevers was measured by using a modified optical readout setup (Fig. 1*A*) as described (11). The cantilever deflection was detected by re-

flection of an external laser beam focused at the cantilever apex. Bending of the cantilever changes the position of the reflected light readout by a position-sensitive detector with subnanometer accuracy. Measurements were performed in a temperature-controlled box. Data acquisition hardware and temperature regulation and a syringe pump for buffer and sample injection were controlled by LABVIEW software. The instrument allows monitoring deflection of all eight cantilevers in parallel in a time-multiplexed manner.

Functionalization of the Cantilever Surface. We used eight-cantilever (0.5 μm thick) silicon arrays fabricated at the IBM Zurich Research Laboratory. The microarray was first cleaned for 2 min (200 W) with plasma (Tepla Giga-Etch 100-E plasma system, Pva Tepla, Asslar, Germany), then incubated for 30 min in 10 mM 2-[methoxypoly(ethyleneoxy)propyl]trimethoxysilane (≈7 ethylene glycol units, ABCR, Karlsruhe, Germany) solution in dry ethanol to create a protein-repellent layer on the lower side of the cantilever. The array was then rinsed with ethanol and dried in air. Afterward, the upper side of the microarray was covered first with a 2-nm Ti layer, followed by a 20-nm Au layer without breaking the vacuum. Deposition of metal layers was performed in an Edwards FL400 electron-beam evaporator (Boc Edwards, Sussex, U.K.) at an evaporation rate of 0.1 nm/s. Cantilever microarrays prepared this way are gold-coated only on the upper side. A polyethylene glycol (PEG)-silane layer is grafted on the lower side. Each microarray was stored in an argon atmosphere for a maximum of 2 days until use.

The protein immobilization was performed by inserting the cantilevers into eight aligned quartz microcapillaries (Garner Glass, Clarmont, CA) with an inner diameter of 150 μm as described (1). With this approach each single cantilever in the array is functionalized separately with scFv fragments C11L34cys (sensor cantilever), G9cys (reference cantilever), or casein (additional reference cantilever) (Fig. 1*B*). The scFv fragments were diluted in HBS buffer (pH 7.5) to a final concentration of 100 μg/ml (3.5 μM). The cantilevers were exposed to the protein solutions for 30–60 min at room temperature. The complete array was rinsed three times with buffer, immersed in 0.5 mg/ml casein in HBS for 1 h at +4°C (to block additional absorption sites), rinsed thoroughly, and finally mounted into the liquid cell of the instrument.

Antigen-Binding Detection. All measurements were carried out in HBST buffer (HBS/0.05% Tween 20, pH 7.5). The buffer was prepared with HPLC water (Fluka), filtrated (0.2-μm filters, Millipore), and degassed. To compare mechanical properties of the individual cantilevers in the array, an assessment of the homogeneity of cantilevers within the array had to be performed before starting binding measurements. For this process, the functionalized cantilever microarray was mounted in the liquid cell containing buffer, and the laser beam was focused at the apex of the cantilever bar. Then the temperature in the cell was increased from 18°C by 2°C for 70 s by using a built-in Peltier element for heating to probe the thermo-mechanical uniformity of the cantilevers. After the liquid cell had cooled down to starting conditions, the maximum deflection magnitude of each cantilever, as caused by the step-like temperature increase, was determined. Only cantilevers that exhibit the same deflection were used for subsequent evaluation of the measurements.

The complete fluidic system with mounted cantilever array was equilibrated for 1 h at 18°C and rinsed several times with 200 μl of buffer to obtain a stable base line. Buffer or protein solutions were injected at a flow rate of 40 μl/min. After injection of 200 μl of antigen solution, the binding was monitored for 1 h, and then the chamber was purged with 800 μl of buffer. To regenerate the array 200 μl of 20 mM glycine buffer (pH 2.8)

was pumped through the cell, which was then immediately rinsed with 800 μl of buffer.

SPR Sensor. SPR measurements were performed with a Biacore 3000 instrument. ScFv fragments at a concentration of 30 μg/ml in HBST buffer (pH 7.5) were directly immobilized on an Au sensor chip (BR-1005-42, Biacore) by using a flow rate of 5 μl/min. Antigen was injected in various dilutions at a flow rate of 10 μl/min.

Ellipsometry. Silicon plates of 0.5×0.5 cm^2 were cleaned with plasma (Tepla Giga-Etch 100-E plasma system, Pva Tepla) for 2 min at 200 W and incubated in 10 mM solution of 2-[methoxy-poly(ethyleneoxy)propyl]trimethoxysilane in ethanol for 30 min. A nonsilanized surface was used as negative control. The plates were rinsed three times with ethanol and dried on air. The thickness of the PEG-silane layer was measured on a variable angle spectroscopic ellipsometer (Woollam, Lincoln, NE). After incubation in 10 mg/ml solution of BSA for 1 h, plates were rinsed with water and dried in a stream of nitrogen. The thickness of the adsorption layer was measured again.

Results

Single microcantilevers are generally known to be susceptible to spurious deflections because of temperature changes, chemical interaction of a coated cantilever with the liquid environment, and slow rearrangement of molecules in the protein multilayer (10, 12, 26, 27). As a result, a base-line drift can be observed during static-mode measurements. Moreover, nonspecific physisorption of antigens on the cantilever surface or nonspecific binding to receptor molecules during measurements may contribute to the drift. To exclude such factors, simultaneous measurement of an *in situ* reference cantilever aligned in the same array as the sensor cantilever is of utmost importance. Therefore, cantilevers coated with similar, but nonbinding, protein constructs can serve as negative *in situ* controls.

We applied two scFv antibody fragments exhibiting specificity toward two different peptides. The scFv fragment C11L34 with specificity to the peptide GCN4(7P14P) derived from the yeast transcription factor GCN4 was isolated from a preimmunized immune library by using ribosome display as described (23). The dissociation constant of this scFv was determined to be $\approx$40 pM. The scFv fragment G9, binding a peptide derived from the amyloid protein PrP, served as a negative control. To immobilize the scFv fragments in a directed orientation on a gold-coated surface, modified constructs with a C-terminal cysteine residue, referred to as C11L34cys and G9cys, were produced.

To characterize the antigen specificity of thiol-modified scFv fragments, both purified constructs were tested for their binding to immobilized peptide GCN4(7P14P) by ELISA. No crossreactivity between the two scFv constructs was observed. Moreover, preincubation of C11L34cys with an excess of free GCN4 peptide inhibited binding of the specific antibody fragment to immobilized peptide completely. This finding additionally confirms a specific binding of purified C11L34cys to antigenic peptide (data not shown).

PEG-Silane Grafting of Silicon Surface. To establish one-sided coating of a cantilever with thiol-containing scFv fragments and prevent their nonspecific adsorption to the bare silicon surface during immobilization, the cantilever's silicon side had to be covered with a layer making the surface inert to proteins. For this purpose, we tested the protein-repelling properties of the low-molecular PEG-terminated silane 2-[methoxypoly(ethyl-eneoxy)propyl]trimethoxysilane (28) by using ellipsometry. The efficiency of protection was estimated by silanization of silicon plates followed by immersion in a concentrated (10 mg/ml) BSA solution. The thickness of the BSA layer adsorbed on bare silicon

plates was determined to be $\approx$1.2 nm, which corroborates earlier published results obtained for BSA adsorbed on silicon at pH 7.4 (29). In contrast, the thickness of the BSA layer additionally adsorbed on PEG-silane-grafted silicon plates was only $\approx$0.5 nm. Thus, PEG-silane treatment reduced protein physisorption significantly. Furthermore, grafting of PEG-silane on a microarray does not influence the later formation of adhesion layers of titanium and gold on the "upper" cantilever surface. The established silanization procedure was applied to the complete cantilever microarrays before their coating with gold.

Antigen Binding Measured with Microcantilever-Based Sensor. To increase the mass of the peptide antigens to allow comparative SPR measurements, a fusion construct was created by the genetic fusion of the antigenic peptide GCN4(7P14P) to an ankyrin (AR) MBP13_6 (30) as a carrier. The final antigen construct, referred to as AR-GCN4, has a molecular mass of $\approx$18 kDa and is thus comparable to the molecular mass of a scFv fragment (28 kDa).

Individual cantilevers of the same array were modified in parallel with C11L34cys (sensor cantilever) or G9cys (reference cantilever). A casein-coated cantilever was used as an additional internal negative control. After immobilization of the cysteine-modified scFv fragments, the cantilever array was immersed in casein solution (Fig. 1B) to prevent additional unspecific adsorption of added antigen during measurements. All measurements were carried out in the liquid cell at 18°C $\pm$ 0.1°C, while the cantilever microarray was immersed in HBS buffer. As a surfactant Tween 20 was added to the buffer to block nonspecific protein–protein interactions (19). Before the binding assay, all eight cantilevers in the array were calibrated to evaluate their mechanical homogeneity (see *Materials and Methods*). The microarray was equilibrated after placing it into the liquid cell to obtain a stable base line.

Different concentrations of antigen (AR-GCN4) were then injected sequentially into the liquid cell. The binding process was monitored for at least 1 h. Then, 800 μl of buffer was flushed through the cell, and the system was equilibrated to reach a stable base line before the next antigen injection. Superimposed differential binding curves were obtained for various concentrations of added antigen (see Fig. 3A). Binding of AR-GCN4 generated a bending of the cantilevers (tensile stress), and the fact that the direction is upward is discussed below. A maximum differential signal of $\approx$50 and 180 nm was obtained for 15- and 300-nM antigen solutions, respectively, and the binding curves leveled off within 30–60 min. No additional binding was detected after injection of buffer. Moreover, the additional reference cantilever functionalized with casein showed an absolute deflection similar to the noncognate G9cys-coated cantilever (data not shown). The data demonstrate that the differential signal observed actually corresponds to a specific binding of antigen to C11L34cys-sensitized cantilevers.

The sensitivity of the experimental device allows one to measure deflection signals of $\approx$3 nm, thus the sensitivity of the technique is in the 1-nM range. Previously, Arntz *et al.* (11) established a detection range of only 1.0 μM for the cardiac marker myoglobin, using a similar instrument. However, in those experiments, anti-myoglobin antibodies ($K_D \approx$1 nM) were immobilized on gold in random orientation by crosslinking of amino groups to a self-assembled monolayer of di-thio-bis-succinimidylundecanoate molecules on a gold surface (31). In the present study, with thiol-containing scFv fragments ($K_D \approx$40 pM) as the receptor layer, the sensitivity was increased by at least a factor of 500. The enhancement of sensitivity cannot only be attributed to higher affinity of the scFv fragments but must also originate from a better orientation and smaller size and thus higher density of the receptor molecules.

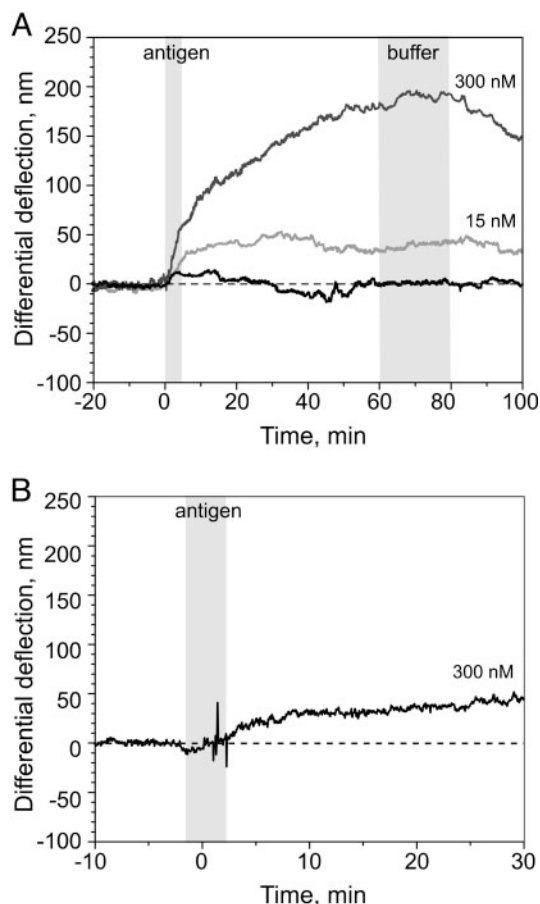An important feature of any biosensor array is its reusability.

Fig. 2. Differential deflection signal (sensing cantilever − reference cantilever) versus time. (*A*) The sensing cantilever was functionalized with a specific scFv fragment (C11L34cys) and the reference cantilever with nonbinding fragment (G9cys). The time periods of injection are visualized as gray stripes. After equilibration in buffer (HBST), sequential injections of buffer (black line), 15 nM (light gray line), and 300 nM (dark gray line) antigen solution (AR-GCN4) were carried out. Binding was followed for 1 h, and then the cell was purged with 800 μl of buffer before the next injection. Raw data for both cantilevers were first normalized by the factor obtained from the thermal cantilever response calibration, then the differential deflection was calculated by subtracting the control cantilevers. (*B*) The functionalized microarray was rinsed with glycine/HCl buffer (pH 2.8) followed by HBST buffer. The antigen (AR-GCN4) was injected at a concentration of 300 nM.

After rinsing the liquid cell with buffer only (Fig. 2*A*), slow dissociation of the antigen was observed. However, the deflection signal did not return to baseline level. This finding is most likely a consequence of the extremely high affinity of the scFv we applied here, which is in the picomolar range. Because of its slow off-rate (32), it is impossible to wash off the antigen completely within hours. We regenerated scFv layers by rinsing the liquid cell with glycine/HCl buffer (pH 2.8) and then equilibrated with buffer until the baseline became stable again. The subsequent injection of 300-nM antigen solution resulted in only 30% of binding ($\approx$50 nm) of the level obtained before the treatment of the array with glycine buffer (Fig. 2*B*). This result implies that either this regeneration was not complete or part of the receptor layer became inactive. scFv fragments might easily lose some of their activity on bare gold under acidic conditions caused by denaturation during the washing step. Interaction of unfolded proteins with the adjacent gold interface could then prevent proper refolding. Future experiments might include new regeneration procedures and application of more robust recombinant molecules with antibody-like properties, such

as ARs (30), as well as protection of gold surface with small organic molecules (33).

The binding of this particular antigen generated absolute tensile stress of the sensor and reference cantilever, resulting in upward bending of the cantilever spring compared with its original position. Absolute tensile deflections have been also observed previously for physical adsorption of different proteins on a gold surface of a single-cantilever array (34–36). Note that the generated surface stress is not a result of mass loaded on a cantilever but of the sum of different processes taking place at the cantilever interface, such as protein–surface and protein–protein interactions whereby the net charge of molecular counterparts plays a key role (35). Therefore, even though the surface is becoming more crowded, changes in surface charge and hydrophilicity of molecules upon formation of antibody–antigen complex result in a tensile stress with an upward movement. Conformational changes within immobilized receptor molecules upon binding of antigenic proteins to the receptor layer may also contribute to this effect. Indeed, a comparison of the crystal structures of C11L34 fragment alone and in complex with GCN4-peptide revealed that, upon peptide binding, the two domains of the scFv undergo a slight rotation relative to each other (32), which may be amplified by the large number of scFvs on the cantilever.

Antigen Binding Measured with a SPR Sensor. To compare the nanomechanical sensor with other label-free measuring techniques, the antigen-binding experiment was performed under the same conditions with a SPR instrument. The scFv fragments C11L34cys and G9cys were immobilized directly on the surface of a Au sensor chip by flushing of 80 μl protein (30 μg/ml), diluted in HBST, through the measuring cells at a flow rate of 5 μl/min. The coating density was $\approx$600 resonance units (RU) for both proteins. Assuming that 1,000 RU corresponds to the surface mass density of 1 ng/mm^2 (37) and the molecular mass of the scFv is 28 kDa, then the amount of protein immobilized on the surface is $\approx$0.6 ng/mm^2 (0.02 pmol/mm^2). A scFv molecule can be approximated as a cylinder with the radius of 3.5 nm (38), therefore a monolayer with the closest molecular packing would have a surface mass density of 1.2 ng/mm^2 (0.04 pmol/mm^2). The SPR data demonstrated that under these functionalization conditions the immobilized molecules occupied $\approx$50% of the available surface.

The antigen was sequentially injected at concentrations of 15 and 300 nM, and the binding process was followed for 30 min. Fig. 3*A* shows an overlay of Biacore sensograms (differential response) for two different antigen concentrations. The maximum reached after 30 min of antigen injection was 50 and 190 RU for 15 and 300 nM antigen solution, respectively. This finding suggests, in a first approximation, that 15% (15 nM antigen) and 50% (300 nM) of the immobilized scFv actually bound an antigen molecule at steady state. The binding signal obtained in this experiment is not as high as it would be expected for fragments of this size (28 kDa) and affinity (40 pM) immobilized on carboxydextran gel layer, using the conventional attachment method. This discrepancy can be explained by the fact that the amount of protein usually adsorbed in a 100-nm-thick hydrogel layer corresponds to the mass of many protein monolayers (39). In contrast, a bare gold surface adsorbs preferentially only one monolayer of protein and therefore can be better compared with our microcantilever experiments.

Regeneration of the chip with glycine/HCl buffer (pH 2.8) and repeated injection of 300-nM antigen dilution resulted in 70% (130 RU) of binding compared with the first injection (Fig. 3*B*). These data are in qualitative agreement with the results obtained with the microcantilever-based sensor and suggest a sensitivity of the microcantilever-based method being equivalent to the one measured in SPR experiments.
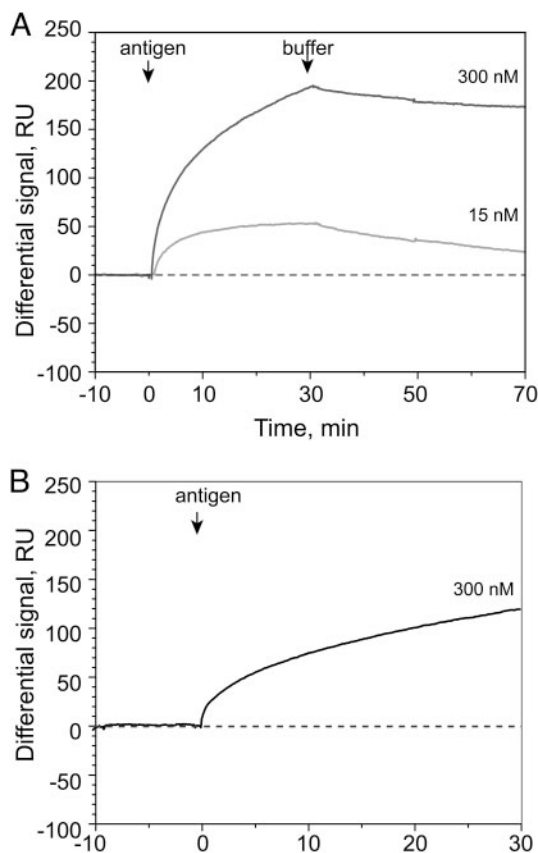
Fig. 3. Sensograms of AR-GCN4 binding to immobilized C11L34cys (the signal obtained for AR-GCN4 binding to G9cys was subtracted). (*A*) The antigen AR-GCN4 was injected at concentrations of 15 nM (light gray line) and 300 nM (dark gray line). Binding was measured for 30 min and dissociation for 40 min. The arrow indicates the beginning of an injection. (*B*) After regeneration of the interface with glycine/HCl buffer (pH 2.8), the antigen was added at a concentration of 300 nM.

Discussion

Because of the label-free detection principle, microcantilever-based sensors have gained interest as a fast method for detection of biomolecules in liquid. The features of the system match major requirements of protein array techniques, such as a miniaturized format, low consumption of analyte, real-time measurements, and the parallelization of the procedure. Implementation of new cantilever-coating technologies, such as inkjet printing (40), and new array formats comprising thousands of cantilevers, like the high-density 2D array reported recently (41), opens up opportunities for scaling up the procedure.

Proper functionalization of sensor surfaces with protein molecules is a challenging, but important, aspect for further development of the method. Efforts are also focused on creation of densely packed homogeneous monolayers of oriented receptors on the interface. In the present study, we investigated the application of scFv antibody fragments as receptor molecules by using a microcantilever-based immunosensor operated in static mode. scFv fragments have been chosen because of their small-size format compared with intact IgG molecules and their ability to be equipped with unpaired cysteines and thus to become immobilized in a site-directed manner. Experiments with Cys-tagged versus untagged scFv (42) and preliminary fluorescence assays using antibody-like molecules, e.g., ARs (43), showed a significant loss in signals for nonthiol-containing proteins, indicating that the molecules are indeed immobilized in a directed manner, and far more efficiently and natively anchored than would be possible by physisorption only. We demonstrated that application of scFv fragments as receptor molecules improved the sensitivity of microcantilever-based detection significantly. Two scFv fragments, C11L34cys and G9cys, with different specificity were attached to gold-coated cantilever surfaces in directed orientation by using a cysteine residue introduced at the C terminus. The binding of antigen AR-GCN4 to immobilized C11L34cys is specific, and the corresponding differential cantilever deflection signal is proportional to the antigen concentration in solution. The current sensitivity of the method is as low as 1 nM (20 ng/ml). These results were directly confirmed by SPR experiments, which demonstrated that the method is comparable in sensitivity. Thus, the threshold of the sensor for protein detection was improved at least 500-fold as compared with previous studies (11, 12) using randomly oriented IgG molecules.

The current sensitivity of a protein microarray for applications in proteomic research has been proposed to be in the picogram range (44), which corresponds to subpicomolar protein concentrations. Recently published microarrays based on scFv antibody fragments and fluorescence reported the sensitivity of protein detection in the femtomolar range (18). In contrast, microcantilever sensors do not require labeling of the antigen and allow unmodified molecules to be measured directly. For alternative label-free immunosensors like quartz crystal microbalance (45) and SPR (46), where recombinant antibody fragments were applied as receptor molecules, detection limits of tumor marker proteins in the range of 10 pg/ml and 10 ng/ml was reported. However, making these systems parallel for array application is rather difficult.

Repeated usage of the array after regenerating it with low-pH buffer resulted in some loss of binding activity, which indicates that C11L34cys scFv fragments immobilized on gold surfaces might undergo unfolding and denaturation upon harsh surface regeneration. To improve the reusability of the sensor, application of very stable scFv fragments suitable for array application should be considered (18, 47, 48). Also, the use of thermodynamically robust recombinant proteins with antibody-like properties, such as ARs (43), may improve the reusability of the sensor.

Microcantilever-based sensors have big potential as biomarker detection tools in proteomic and genomic research and medical diagnostics. Detailed information about the expression level of both the mRNA and the corresponding protein is needed to understand a complex biological system. Cantilever arrays provide a platform for the development of multifunctional assays enabling parallel detection of different biomolecules, such as mRNA, DNA, and proteins.

1. Lang, H. P., Hegner, M. & Cerber, C. (2005) *Materials Today* **8,** 30–36.
2. Lavrik, N. V., Sepaniak, M. J. & Datskos, P. G. (2004) *Rev. Sci. Instrum.* **75,** 2229–2253.
3. Hood, L., Heath, J. R., Phelps, M. E. & Lin, B. (2004) *Science* **306,** 640–643.
4. Ferrari, M. (2005) *Nat. Rev.* **5,** 161–171.
5. Wu, G., Ji, H., Hansen, K., Thundat, T., Datar, R., Cote, R., Hagan, M. F., Chakraborty, A. K. & Majumdar, A. (2001) *Proc. Natl. Acad. Sci. USA* **98,** 1560–1564.
6. Fritz, J., Baller, M. K., Lang, H. P., Rothuizen, H., Vettiger, P., Meyer, E., Guntherodt, H., Gerber, C. & Gimzewski, J. K. (2000) *Science* **288,** 316–318.

7. McKendry, R., Zhang, J., Arntz, Y., Strunz, T., Hegner, M., Lang, H. P., Baller, M. K., Certa, U., Meyer, E., Guntherodt, H. J. & Gerber, C. (2002) *Proc. Natl. Acad. Sci. USA* **99,** 9783–9788.

8. Savran, C. A., Knudsen, S. M., Ellington, A. D. & Manalis, S. R. (2004) *Anal. Chem.* **76,** 3194–3198.

9. Huber, F., Hegner, M., Gerber, C., Güntherodt, H.-J. & Lang, H. P. (2005) *Biosens. Bioelectron.*, in press.

10. Wu, G., Datar, R. H., Hansen, K. M., Thundat, T., Cote, R. J. & Majumdar, A. (2001) *Nat. Biotechnol.* **19,** 856–860.

11. Arntz, Y., Seelig, J. D., Lang, H. P., Zhang, J., Hunziker, P., Ramseyer, J. P., Meyer, E., Hegner, M. & Gerber, C. (2003) *Nanotechnology* **14,** 86–89.

12. Raiteri, R., Grattarola, M., Butt, H.-J. & Skladal, P. (2001) *Sensors Actuators B* **79,** 115–126.

13. Peluso, P., Wilson, D. S., Do, D., Tran, H., Venkatasubbaiah, M., Quincy, D., Heidecker, B., Poindexter, K., Tolani, N., Phelan, M., *et al.* (2003) *Anal. Biochem.* **312,** 113–124.

14. Zhou, J., Chen, S. & Jiang, S. (2003) *Langmuir* **19,** 3472–3478.

15. Karyakin, A. A., Presnova, G. V., Rubtsova, M. Y. & Egorov, A. M. (2000) *Anal. Chem.* **72,** 3805–3811.

16. Kanno, S., Yanagida, Y., Haruyama, T., Kobatake, E. & Aizawa, M. (2000) *J. Biotechnol.* **76,** 207–214.

17. Nugaeva, N., Gfeller, K. Y., Backmann, N., Lang, H. P., Düggelin, M. & Hegner, M. (2005) *Biosens. Bioelectron.*, in press.

18. Wingren, C., Steinhauer, C., Ingvarsson, J., Persson, E., Larsson, K. & Borrebaeck, C. A. K. (2005) *Proteomics* **5,** 1281–1291.

19. Brogan, K. L., Shin, J. H. & Schoenfisch, M. H. (2004) *Langmuir* **20,** 9729–9735.

20. Plückthun, A. (1990) *Nature* **347,** 497–498.

21. Winter, G., Griffiths, A. D., Hawkins, R. E. & Hoogenboom, H. R. (1994) *Annu. Rev. Immunol.* **12,** 433–455.

22. Hanes, J. & Plückthun, A. (1997) *Proc. Natl. Acad. Sci. USA* **94,** 4937–4942.

23. Hanes, J., Jermutus, L., Weber-Bornhauser, S., Bosshard, H. R. & Plückthun, A. (1998) *Proc. Natl. Acad. Sci. USA* **95,** 14130–14135.

24. Krebber, A., Bornhauser, S., Burmester, J., Honegger, A., Willuda, J., Bosshard, H. R. & Plückthun, A. (1997) *J. Immunol. Methods* **201,** 35–55.

25. Hanes, J., Schaffitzel, C., Knappik, A. & Plückthun, A. (2000) *Nat. Biotechnol.* **18,** 1287–1292.

26. Grogan, C., Raiteri, R., O'Connor, G. M., Glynn, T. J., Cunningham, V., Kane, M., Charlton, M. & Leech, D. (2002) *Biosens. Bioelectron.* **17,** 201–207.

27. Moulin, A. M., O'Shea, S. J. & Welland, M. E. (2000) *Ultramicroscopy* **82,** 23–31.

28. Papra, A., Gadegaard, N. & Larsen, N. B. (2001) *Langmuir* **17,** 1457–1460.

29. Freeman, N. J., Peel, L. L., Swann, M. J., Cross, G. H., Reeves, A., Brand, S. & Lu, J. R. (2004) *J. Phys. Condens. Matter* **16,** 2493–2496.

30. Binz, H. K., Amstutz, P., Kohl, A., Stumpp, M. T., Briand, C., Forrer, P., Grütter, M. G. & Plückthun, A. (2004) *Nat. Biotechnol.* **22,** 575–582.

31. Wagner, P., Hegner, M., Kernen, P., Zaugg, F. & Semenza, G. (1996) *Biophys. J.* **70,** 2052–2066.

32. Zahnd, C., Spinelli, S., Luginbühl, B., Amstutz, P., Cambillau, C. & Plückthun, A. (2004) *J. Biol. Chem.* **279,** 18870–18877.

33. Schwesinger, F., Ros, R., Strunz, T., Anselmetti, D., Güntherodt, H.-J., Honegger, A., Jermutus, L., Tiefenauer, L. & Plückthun, A. (2000) *Proc. Natl. Acad. Sci. USA* **97,** 9972–9977.

34. Dutta, P., Tipple, C. A., Lavrik, N. V., Datskos, P. G., Hofstetter, H., Hofstetter, O. & Sepaniak, M. J. (2003) *Anal. Chem.* **75,** 2342–2348.

35. Moulin, A. M., O'Shea, S. J., Badley, R. A., Doyle, P. & Welland, M. E. (1999) *Langmuir* **15,** 8776–8779.

36. Lavrik, N. V., Tipple, C. A., Sepaniak, M. J. & Datskos, P. G. (2001) *J. Biomed. Microdevices* **3,** 35–44.

37. O'Shannessy, D. J., Brigham-Burke, M., Soneson, K. K., Hensley, P. & Brooks, I. (1993) *Anal. Biochem.* **212,** 457–468.

38. Howell, S., Kenmore, M., Kirkland, M. & Badley, R. A. (1998) *J. Mol. Recognit.* **11,** 200–203.

39. Stenberg, E., Persson, B., Roos, H. & Urbaniczky, C. (1991) *J. Colloid Interface Sci.* **143,** 513–526.

40. Bietsch, A., Zhang, J., Hegner, M., Lang, H. P. & Gerber, C. (2004) *Nanotechnlogy* **15,** 873–880.

41. Despont, M., Drechsler, U., Yu, R. R., Pogge, B. H. & Vettiger, P. (2004) *J. Microelectromech. Syst.* **13,** 895–901.

42. Ros, R., Schweisinger, F., Anselmeti, D., Kubon, M., Schäfer, R., Plückthun, A. & Tiefenauer, L. (1998) *Proc. Natl. Acad. Sci. USA* **95,** 7402–7405.

43. Binz, H. K., Stumpp, M. T., Forrer, P., Amstutz, P. & Plückthun, A. (2003) *J. Mol. Biol.* **332,** 489–503.

44. Kuznezow, W. & Hoheisel, J. D. (2002) *BioTechniques* **33,** 14–23.

45. Kurosawa, S., Nakamura, M., Park, J.-W., Aizawa, H., Yamada, K. & Hirata, M. (2004) *Biosens. Bioelectron.* **20,** 1134–1139.

46. Huang, L., Reekmans, G., Saerens, D., Friedt, J.-M., Frederix, F., Francis, L., Muyldermans, S., Campitelli, A. & Van Hoof, C. (2005) *Biosens. Bioelectron.* **21,** 483–490.

47. Söderlind, E., Strandberg, L., Jirholt, P., Kobayashi, N., Alexeiva, V., Aberg, A.-M., Nillson, A, Jansson, B., Ohlin, M., Wingren, C., *et al.* (2003) *Nat. Biotechnol.* **18,** 852–856.

48. Knappik, A., Ge, L., Honegger, A., Pack, P., Fischer, M., Wellnhofer, G., Hoess, A., Wölle, J., Plückthun, A. & Virnekäs, B. (2000) *J. Mol. Biol.* **296,** 57–86.